going from stagnation pressures of 100 to 200 psia and lower Mach numbers, and also include data with thicker boundary layers upstream of the interactions.

To calculate the distribution of the heat-transfer coefficient, the energy Eq. (1) can be integrated along the wall, since the heat flux is related to the energy thickness by Eqs. (2) and (3), to obtain the energy thickness distribution once the freestream flow variables and wall temperature are specified (see Ref. 3 for such a calculation upstream, within and downstream of some of the interactions presented herein).

Attention is now focused on the interpretation of the prediction when it is applied to other experimental data at shock impingement locations where there appears to be similarity between the measured heat-transfer and pressure changes. For example, Sayano[1] has given the empirical relation $(h_2/h_1) = (p_2/p_1)^{0.8}$ from his results and, more recently Markarian,[10] in reviewing some measurements, suggested a slightly stronger empirical power law dependence with the exponent 0.85. It is useful here to recast Eq. (4) in terms of a pressure change. For isentropic flow, the variation of the mass flux and group from Eq. (4) with pressure ratio is shown in Fig. 3 in nondimensional form. Although over the large Mach number range shown (1–10) there is no particular power law fit, the values agree reasonably well in the supersonic range from about 2–6 with the dashed curve shown. This correspondence implies the following relationship between the change in heat-transfer coefficient and pressure from Eq. (4):

$$h_2/h_1 \cong (p_2/p_1)^{0.85} \tag{5}$$

The prediction from Eq. (5) is compared with experimental measurements in Fig. 2. The agreement is satisfactory, even in the hypersonic flow regime where the prediction might not be expected to agree as well by inference from Fig. 3. This may be partly due to the smaller increase in the group $(\rho_e u_e)_2/(\rho_e u_e)_1[(T_{e_2}/T_{e_1})]^{3/4}$ across shock waves than the corresponding isentropic flow values when the shock waves are stronger, i.e., $\Delta p/p \cong \gamma M\sigma$. For example, for isentropic flow in the hypersonic limit $M_e \to \infty$, $[(\rho u/\rho_0 a^*)][(T/T_0)]^{3/4} \alpha[(p/p_0)]^n$ where $n = 1/\gamma + (\frac{3}{4})(\gamma - 1/\gamma) = 0.93$ for $\gamma = 1.4$. Also, it could be associated with the correction for compressibility effects as contained in Eq. (2) that partially led to the $T^{3/4}$ dependence in Eq. (4). This correction may be too large in hypersonic flows, e.g., in Eq. (2) as $M_e \to \infty$, $(T_e/T_{aw}) \to 0$.

For compression corners, Markarian[10] has shown some results of other investigations in the representation of Fig. 2. Although there is some uncertainty in the structure of the boundary layer just upstream of the corner for some of the data, i.e., transitional or just turbulent in these external flows, and in the resolution of the peak heat transfer downstream, the results do appear to agree with the indication of Eq. (5), as also do the present results obtained with a curved compression corner (Fig. 2).

References

[1] Sayano, S., Bausch, H. P., and Donnelly, R. J., "Aerodynamic Heating Due to Shock Impingement on a Flat Plate," SM-41331, Aug. 1962, McDonnell-Douglas Aircraft Co., Santa Monica, Calif.

[2] Levin, V. and Fabish, T. J., "Thermal Effects of Shock Wave Turbulent Boundary Layer Interaction at Mach Numbers 3 and 5," 62H-795, Nov. 1962, North American Aviation, Columbus, Ohio.

[3] Back, L. H., Cuffel, R. F., and Massier, P. F., "Experimental Convective Heat Transfer and Pressure Distributions and Boundary Layer Thicknesses in Turbulent Flow Through a Variable Cross-Sectional Area Channel," *4th International Heat Transfer Conference Proceedings*, Paris, France, Vol. II FC2.1, 1970, pp. 1–14.

[4] Back, L. H., Massier, P. F., and Cuffel, R. F., "Flow Phenomena and Convective Heat Transfer in a Conical Supersonic Nozzle," *Journal of Spacecraft and Rockets*, Vol. 4, No. 8, Aug. 1967, pp. 1040–1047.

[5] Back, L. H., Cuffel, R. F., and Massier, P. F., "Laminarization of a Turbulent Boundary Layer in Nozzle Flow—Boundary Layer and Heat Transfer Measurements with Wall Cooling," to be published in ASME *Journal of Heat Transfer*.

[6] Ambrok, G. S., "Approximate Solution of Equations for the Thermal Boundary Layer with Variations in Boundary Layer Structure," *Soviet Physics*, Vol. 2 (II), 1957, pp. 1979–1986.

[7] Kutateladze, S. S. and Leontev, A. I., "Drag Law in a Turbulent Flow of a Compressible Gas and the Method of Calculating Friction and Heat Exchange," *Akademii Nauk, Belorussk*, SSR, Minsk, Jan. 1961, pp. 23–27; translated and issued by Technical Information and Library Services, Dec. 1961, Ministry of Aviation, London, England.

[8] Romanenko, P. N., Leontev, A. I., and Oblivin, A. N., "Investigation on Resistance and Heat Transfer of Turbulent Air Flow in Axisymmetrical Channels with Longitudinal Pressure Gradient," *International Journal of Heat and Mass Transfer*, Vol. 5, June 1962, pp. 541–557.

[9] Back, L. H. and Cuffel, R. F., "Turbulent Boundary Layer and Heat Transfer Measurements Along a Convergent-Divergent Nozzle," to be published.

[10] Markarian, C. F., "Heat Transfer in Shock Wave-Boundary Layer Interaction Regions," TP 4485, Nov. 1968, Naval Weapons Center, China Lake, Calif.

[11] Magnan, J. D., Jr. and Spurlin, C. J., "Investigation of Flow Field Interference Caused by Shock Impingement on a Flat Plate at Mach Numbers of 6, 8, and 10," TR-66-85, April 1966, Arnold Engineering Development Center, Arnold Air Force Base, Tenn.

[12] Gulbran, C. E. et al., "Heating in Regions of Interfering Flow Fields, Part III: Two-Dimensional Interaction Caused by Plane Shocks Impinging on Flat Plate Boundary Layers," AFFDL-TR-65-49, Pt. III, March 1967, The Boeing Company, Wright-Patterson Air Force Base, Ohio.

[13] Comfort, E. and Todisco, A., "Experimental Investigation of Two Shock Wave Boundary Layer Interaction Configurations," AIAA Paper 69-8, New York, 1969.

Turbulent Boundary-Layer Computations Based on an Extended Mixing Length Approach

Y. Y. CHAN*

National Aeronautical Establishment, Ottawa, Canada

IN the recent development of computational methods for turbulent boundary layers[1,2] Prandtl's mixing length concept is again widely used to correlate the turbulent shear stress to the local mean flow of the boundary layer. In the methods of Patankar and Spalding,[3] Beckwith and Bushnell,[4] and Pletcher[5] the mixing length is correlated to the local thickness of the boundary layer and the correlation function for flow passed a flat plate is usually assumed for general uses. The drawback of these methods is in that the flat plate correlation represents a reasonable approximation only for flows with moderate pressure gradients,[6] but is not necessarily true for flows with large pressure gradients, especially for adverse pressure gradients. By directly relating the mixing length to the mean flow, these mean-field methods do not consider the development of the turbulent field explicitly and thus are not very successful in predicting highly nonequilibrium flows. In the method of McDonald and Camarata,[7] these shortcomings are overcome. The mixing length is no longer correlated directly to the mean-flow field of the boundary layer, but is calculated by the integral turbulent kinetic energy equation, thus the history of the turbulent state is considered explicitly and the mixing length correlation is allowed to vary as the turbulent boundary layer develops. This method is similar to the approach of Bradshaw

Received February 16, 1970; revision received April 30, 1970.

* Associate Research Officer, High Speed Aerodynamics Section. Member AIAA.

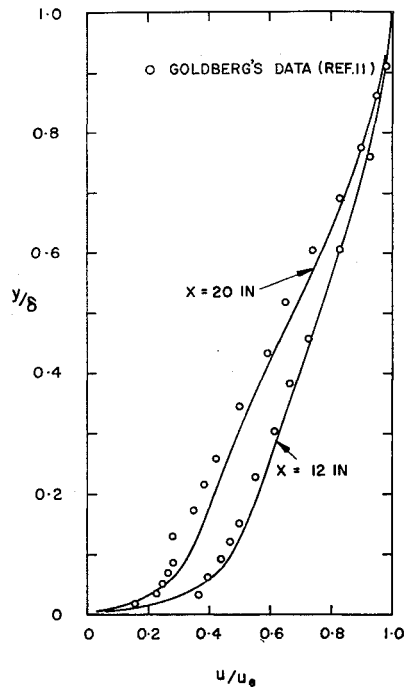

Fig. 1 Calculated velocity profiles at two stations along the body.

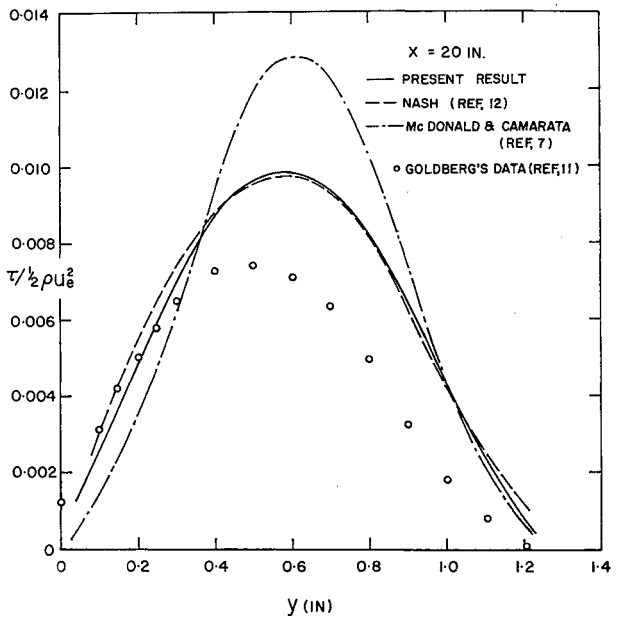

Fig. 3 Comparison of turbulent shear stress distributions at $x = 20$ in.

et al.[8] with the exception that by using an integral formulation of the turbulent kinetic energy equation, the pressure-velocity diffusion process is eliminated and an assumption as to the distribution of mixing length across the boundary layer is made. For an integral formulation, it is necessary to assume velocity profiles in the process of solution. The integral properties of the boundary layer that are evaluated directly from the resulting velocity profiles are predicted satisfactory. However, the turbulent shear stress that is related to the square of the derivative of the velocity profile and thus more sensitive to the profile shapes is predicted with less accuracy. This is because the assumed velocity profile may not reproduce the actual distribution of velocity close enough. The resulting poor prediction of the turbulent shear stress can readily be improved if the equations of the mean-flow field are solved in their differential forms. The velocity distribution will then be a part of the solutions and

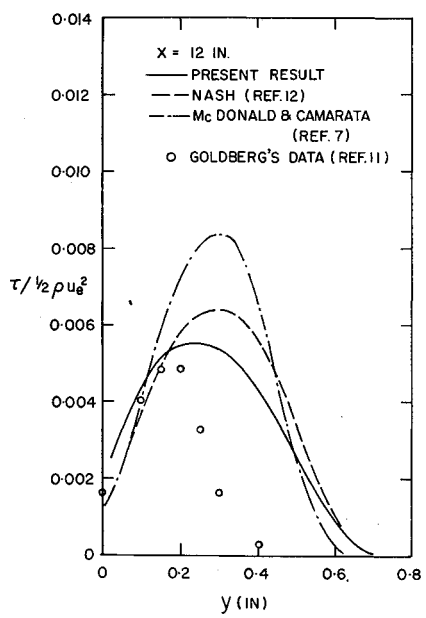

Fig. 2 Comparison of turbulent shear stress distributions at $x = 12$ in.

the accuracy will depend only on the assumed model of the turbulent state. In addition this differential formulation will allow us to assess the extended mixing length concept by comparison with other differential methods with different models for the turbulent shear stress.

This differential formulation is carried out in detail in Ref. 8 and a brief description of the computation technique and some results are given herein. The two-dimensional boundary layer equations of an incompressible flow are transformed in terms of a stream function

$$[(1 + \epsilon_T/\mu)f_{\eta\eta}]_\eta + ff_\eta + 2\xi(u_{e\xi}/u_e)(1 - f_\eta^2) = 2\xi(f_\eta f_{\xi\eta} - f_\xi f_{\eta\eta}) \quad (1)$$

where the coordinate transformation is

$$d\xi = (u_e/\nu)dx,\ d\eta = [u_e/\nu(2\xi)^{1/2}]dy$$

and the nondimensional velocity component

$$u/u_e = f_\eta$$

The boundary conditions are as follows

$$f_\eta(\xi,0) = 0, f(\xi,0) = 0 \quad \text{with zero injection or suction}$$

$$f_\eta \to 1 \text{ as } \eta \to \infty$$

The eddy viscosity ϵ_T is defined by the relation

$$-\rho[u'v'] = \epsilon_T \partial u/\partial y$$

Equation (1) with the boundary condition is solved numerically by an implicit finite difference method. The equation is linearized in a form suitable for an iterative calculation[9] as

$$[(1 + \epsilon_T/\mu)^{(p-1)}F_{\eta\eta}^{(p)} + (\epsilon_T/\mu)_\eta^{(p-1)}F_\eta^{(p)}] + f^{(p-1)}F_\eta^{(p)} + 2\xi(ue_\xi/u_e)(1 - F^{(p-1)}F^{(p)}) = 2\xi(F^{(p-1)}F_\xi^{(p)} - f_{\xi e}^{(p-1)}F_\eta^{(p)})$$

where $F = f_\eta$ and

$$f = \int_0^\eta F d\eta$$

The superscripts (p) and $(p-1)$ denote the order of the iteration process. The equation is now of second order and is

solved for the function F. The derivatives and integration in the η direction are expressed by three point difference formula, the derivative in the ξ direction is approximated by a forward difference and the function F is written in terms of the values of two adjacent points in the ξ direction as

$$F = \lambda F_{i,j+1} + (1 - \lambda)F_{i,j}$$

where λ is a weighting factor which can be suitably adjusted for improving the convergency of the iteration scheme. Then a system of linear algebraic equation results and can be solved by an elimination method.

Close to the wall, van Driest's laminar damping for the laminar sublayer is assumed. Thus the mixing length variation for the sublayer is

$$l = 0.41y[1 - \exp(-y/A)] \tag{2}$$

where

$$A = 26\nu(\rho/\tau_{\max})^{1/2}$$

The $\tau_{\max}$ is the maximum shear stress occurred in the laminar sublayer.[9] The mixing length is assumed to increase monotonically to a constant value in the outer portion of the boundary layer. A scaling length that can be related to the value of mixing length in the outer portion of the boundary layer, is computed from the integral turbulent kinetic energy equation. The turbulent energy equations in integral form is[7]

$$\frac{1}{2}\frac{d}{dx}\int_0^\delta u[q]^2dy = \int_0^\delta -[u'v']\frac{\partial u}{\partial y}\,dy - \int_0^\delta \epsilon dy$$

which can be related to the turbulent shear stress by the assumptions

$$-[u'v'] = k[q]^2,\ \epsilon = \frac{(-[u'v'])^{3/2}}{L},\ -[u'v'] = l^2\left(\frac{\partial u}{\partial y}\right)^2$$

and integrated to yield

$$t = \frac{1}{\rho_e u_e{}^3\phi_1}\left[(\rho_e u_e{}^3 t\phi_1)_0 + 2k\int_{x_0}^x \rho_e u_e{}^3\phi_2 dx\right] \tag{3}$$

with

$$\phi_1 = \int_0^{\delta/t}\left(\frac{l}{t}\right)^2\frac{u}{u_e}\left(\frac{\partial u/u_e}{\partial y/t}\right)^2 d\left(\frac{y}{t}\right)$$

$$\phi_2 = \int_0^{\delta/t}\left(\frac{l}{t}\right)^2\left(\frac{\partial u/u_e}{\partial y/t}\right)^3\left(1 - \frac{l}{L}\right)d\left(\frac{y}{t}\right)$$

where t is the scaling length which is proportional to the value of mixing length at infinity. With the assumed form of mixing length distribution across the boundary layer, Eq. (3) provides the means to compute the state of turbulence required in the momentum equation and thus forms a part in the iteration process of the computation. The empirical quantities are chosen as

$$k = 0.15,\ L/\delta = 0.09\tanh(4.56y/\delta)$$

$$l/t = \tanh(0.41y/t)$$

based on correlations of experimental data[7,9,12] and the scaling length t is related to the mixing length at infinity.

The example given in Ref. 7, Goldberg's experiment case 3,[11] is recomputed by the present formulation and some results are given herein for comparison with those of Ref. 7. In this experiment, the boundary layer is driven by a steep adverse pressure gradient close to separation and then recovered by removing the pressure gradient. This highly nonequilibrium case provides critical tests to the adequacy of the prediction method. In the present computation, all computed integral properties agree very well with the experimental data and the details are given in Ref. 9. As the prediction of velocity profiles and the distributions of turbulent shear stresses are emphasized in the present formulation, only these results are shown herein. Figure 1 shows the computed velocity profiles in comparison with experimental data at two stations along the body and good agreement is obtained. The turbulent shear stress distribution at $x = 12$ in. is shown in Fig. 2. The result calculated by Nash[12] using Bradshaw's theory is also shown in the figure, and is considered to be more accurate as in his formulation, the turbulent energy equation is solved in its differential form. Thus the turbulent diffusion process which does not appear in the integral form of the equation, is fully considered and in addition, the assumptions as to the distributions of some fluctuating quantities are also avoided. At this station, the present result is slightly lower than that of Nash's and improves greatly on that of Ref. 7. A similar comparison at $x = 20$ in. is shown in Fig. 3. The present result agrees very well with that of Nash's and again improves on the result of Ref. 7. The experimental data are consistently lower than the predicting results as also noted by Nash.

In concluding, it is shown by comparison with experimental data and other theoretical results that the present differential formulation in cooperating with the extended mixing length concept originated by McDonald and Camarata provides an accurate method of computation for turbulent boundary layers in an incompressible flow with strong pressure gradients. Although the present differential technique is more involved in computation than the integral method of Ref. 7, this disadvantage is offset by the higher accuracy of the predicting results, especially for the distributions of mean velocities and the turbulent shear stresses.

References

[1] Kline, S. J. et al., ed., *Proceedings Computation of Turbulent Boundary Layers—1968*, AFOSR-IFP-Stanford Conference, Vol. 1, Stanford Univ., Stanford, Calif.

[2] Bertram, M. H., ed., *Compressible Turbulent Boundary Layers*, NASA SP-216, Dec. 1968.

[3] Patankar, S. V. and Spalding, D. B., *Heat and Mass Transfer in Boundary Layers*, Morgan-Grampian, London, 1967.

[4] Bushnell, D. M. and Beckwith, I. E., "Calculation of Nonequilibrium Hypersonic Turbulent Boundary Layers and Comparisons with Experimental Data," AIAA Paper 69-684, San Francisco, Calif., 1969.

[5] Pletcher, R. H., "On a Finite-Difference Solution for the Constant-Property Turbulent Boundary Layer," *AIAA Journal*, Vol. 7, No. 2, Feb. 1969, pp. 305–311.

[6] Maise, G. and McDonald, H., "Mixing Length and Kinematic Eddy Viscosity in a Compressible Boundary Layer," *AIAA Journal*, Vol. 6, No. 1, Jan. 1968, pp. 73–79.

[7] McDonald, H. and Camarata, F. J., "An Extended Mixing Length Approach for Computing the Turbulent Boundary Layer Development" *Proceedings Computation of Turbulent Boundary Layers—1968*, AFOSR-IFP-Stanford Conference Vol. 1, Aug. 1968, Stanford Univ., Stanford, Calif., pp. 83–98.

[8] Bradshaw, P., Ferriss, D. H., and Atwell, N. P., "Calculation of Boundary Layer Development Using the Turbulent Energy Equation," *Journal of Fluid Mechanics*, Vol. 28, Pt. 3, 1967, pp. 593–616.

[9] Chan, Y. Y., "Comparison of Several Mixing Length Models for Turbulent Boundary Layer Computations," Aero. Report LR-531, March 1970, National Research Council of Canada.

[10] Sells, C. C. L., "Two-dimensional Laminar Compressible Boundary Layer Programme for a Perfect Gas," TR 66243, Aug. 1966, Royal Aircraft Extablishment.

[11] Goldberg, P., "Upstream History and Apparent Stress in Turbulent Boundary Layers," Rept. 85, May 1966, Gas Turbine Lab., Massachusetts Institute of Technology.

[12] Nash, J. F., "A Finite-Difference Method for the Calculation of Incompressible Turbulent Boundary Layers in Two-dimensions," ER-9655, Feb. 1968, Lockheed-Georgia Co., Marietta, Ga.